Leckie, R.M., Sigurdsson, H., Acton, G.D., and Draper, G. (Eds.), 2000
Proceedings of the Ocean Drilling Program, Scientific Results, Vol. 165

12. SYNTHETIC SEISMOGRAM GENERATION AND SEISMIC FACIES TO CORE LITHOLOGY CORRELATION FOR SITES 998, 1000, AND 1001[1]

A.D. Cunningham[2] and A.W. Droxler[3]

ABSTRACT

One-dimensional synthetic seismograms are constructed from velocity and density measurements taken during Ocean Drilling Program (ODP) Leg 165 at Sites 998, 1000, and 1001. The synthetic seismograms facilitate correlation of single-channel seismic (SCS) reflection profiles acquired aboard the *Cape Hatteras* and *Maurice Ewing* with core lithologies obtained during ODP drilling of the three sites. Visual correlation between the synthetic seismograms and SCS data is generally good. Several high-amplitude reflectors in the seismic data correlate with high-amplitude events in the synthetic seismogram and are the result of changes in velocity and/or density of the cored interval. Variations in SCS facies correlate with changes in core lithologies.

INTRODUCTION

Drilling during Ocean Drilling Program (ODP) Leg 165 recovered core, velocity, and density information that can be used to correlate core lithologies and ages of sedimentary units with high-resolution single-channel seismic profiles crossing Sites 998, 1000, and 1001 (Fig. 1). Because predictions of velocities with depth derived from the empirical velocity vs. depth functions of Carlson et al. (1986) do not match either laboratory or log velocity measurements at these sites, a correlation of core to seismic data using such a function will have significant error. In the absence of check-shot survey data or vertical seismic profiles, synthetic seismograms provide a means to correlate seismic facies and seismic reflections with core lithologies.

Synthetic seismograms were constructed using velocity and density data obtained during Leg 165. Velocity and density estimates were acquired from downhole sonic and density logs and from physical properties measurements of recovered cores (Sigurdsson, Leckie, Acton, et al., 1997). Sonic and density log measurements were not available in the top and bottom portions of the hole, however. Core-derived velocity and density measurements can be merged with sonic and density logs to create a relatively continuous velocity and density profile extending from the seafloor to near the base of the hole. Synthetic seismograms were created for Sites 998, 1000, and 1001 from the velocity and density profiles. These synthetic seismograms are spliced into single-channel seismic reflection profiles crossing the sites and a comparison is made between core lithologies and seismic facies.

DATA SETS

Single-channel seismic reflection profiles were collected prior to drilling of ODP Leg 165. A 1992 seismic survey over Site 1000 was conducted aboard the *Cape Hatteras*. Seismic data over Sites 998 and 1001 were collected as part of a 1994 ODP site survey aboard the *Maurice Ewing*. These seismic sections are compared with results generated from data accumulated during Leg 165. These data include physical properties measurements of velocity and density, downhole logs, and lithostratigraphic core descriptions (Sigurdsson, Leckie, Acton, et al., 1997).

During April and May of 1992, research Cruise CH9204 aboard the *Cape Hatteras* was completed as part of a study of Pedro Channel and Serranilla Basin on the northern Nicaraguan Rise. Over 2300 km of digital, high-resolution single-channel seismic reflection (SCS) data was obtained in Pedro Channel using an 80-in^3 GI air gun from Seismic Systems Inc. as the seismic source. The GI gun was fired every 7–10 s at a ship speed of 5.5 kt and digitized at a 1 ms sampling rate, using the Rice University Elics/Delph 1 system. Navigation for the SCS data consists of Global Positioning System (GPS) fixes roughly every 30 shots.

The single-channel seismic reflection data sets over Sites 998 and 1001 were collected during research Cruise EW9417 in December of 1994 aboard the *Maurice Ewing*. Approximately 270 km of SCS data in the vicinity of Site 998 and 335 km of SCS data near Site 1001 were acquired using two 80-in^3 SSI water guns fired every 10 s as an energy source and digitized at a 1-ms sampling rate with the Rice University Elics/Delph 2 acquisition system. GPS fixes are available at each shotpoint.

Processing and display of the SCS data was completed in the Rice University Geology and Geophysics Department. ProMAX Version 6.0 on an IBM RS6000 was used to process the data. A typical processing flow included trace equalization, hand statics corrections, removal of noisy traces, band-pass filtering (25–50–200–400 Hz), 200-ms Automatic Gain Control (AGC), water bottom mute, and variable displays. Because the water guns used in the EW9417 data acquisition were out of phase, a predictive deconvolution with an 80-ms operator length was applied to the EW9417 data to compress the multi-peaked source signal. The dominant frequency of both seismic data sets is ~100 Hz and results in a theoretical seismic resolution of 4–10 m (based on sediment velocities of 1600–4000 m/s.

Sonic and density logs as well as physical properties measurements from Leg 165 (Sigurdsson, Leckie, Acton, et al., 1997) were used in creating the synthetic seismograms. Physical properties measurements of velocity were obtained using the digital sonic velocimeter (DSV) on unconsolidated sediments and the Hamilton Frame on samples that were too consolidated for use on the DSV (Sigurdsson, Leckie, Acton, et al., 1997). Wet bulk density measurements were collected as part of index properties measurements. Descriptions of the sediment recovered during coring operations were compared with reflection patterns on the synthetic seismogram and SCS seismic facies. Biostratigraphy for the cored intervals provided age control.

[1]Leckie, R.M., Sigurdsson, H., Acton, G.D., and Draper, G. (Eds.), 2000. *Proc. ODP, Sci. Results,* 165: College Station, TX (Ocean Drilling Program).

[2]BP Amoco, 501 Westlake Park Blvd., Houston, TX 77253-3092, U.S.A. cunninad@bp.com

[3]Department of Geology and Geophysics, Rice University, 6100 South Main Street, Houston, TX 77005-1892, U.S.A.

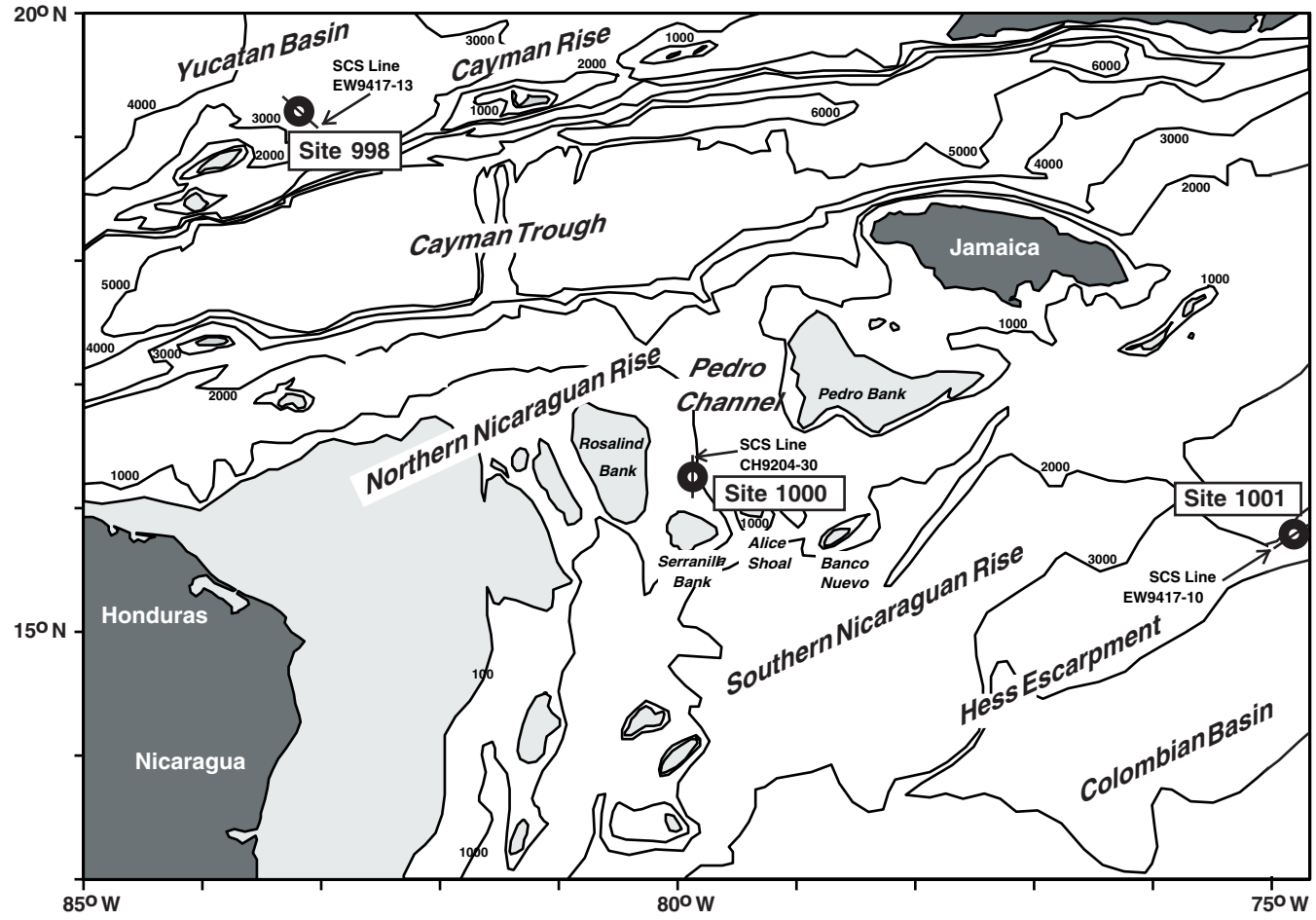

Figure 1. Location map for Sites 998, 1000, and 1001. Contour interval = 1000 m.

SYNTHETIC SEISMOGRAM GENERATION

During ODP Leg 165, sonic and density logs were collected. The depth-corrected logs were then obtained from the Borehole Research Group at the Lamont-Doherty Earth Observatory. After parsing and reformatting the logs, each log was examined individually, looking for obviously erroneous values in velocity or density that would create artificial acoustic impedance contrasts and could result in the creation of false reflections on the synthetic seismograms. The far-spaced sonic log was used at Sites 1000 and 998, but the near-spaced sonic had to be used at Site 1001 because of the poor quality of the far-spaced sonic log. Density logs of reasonably good quality were available for all three sites.

In general, the downhole sonic and density log measurements matched the values obtained from physical properties core measurements (Figs. 2, 3, 4, 5, 6.). The only major variance was in the Site 1001 sonic measurements (Fig. 7). The measurements recorded in this log were all significantly lower than those measured in physical properties. The trend of the log values does mimic the general trend of the physical properties measurements. The sonic log could not be used with the physical properties data because the gap between the two data sets would create an artificial impedance contrast at the data merge point. To obtain a proper merge of the physical properties and sonic log data, the physical properties data set needed to be divided by a constant factor of 1.125. The resultant data shows significantly better agreement between the sonic log data and the physical properties velocity data (Fig. 8). Thus, modified physical properties data were used as part of the velocity profile in creating the synthetic seismogram. Synthetic seismograms created using this velocity log correlate well with the seismic data over the site.

Because of the possibility that the physical properties measurements yielded more accurate values than the sonic log measurements, a second velocity profile was created in which the sonic log values were multiplied by 1.125 rather than dividing the physical properties data by 1.125. Synthetic seismograms were also created using this second velocity profile as well. This second synthetic seismogram did not tie well with the SCS profile at Site 1001, and resulted in synthetic horizons that appear significantly shallower in the synthetic than in the seismic data. A probable reason for the mistie between the synthetic seismogram and the seismic data is that the velocities used in this time-depth conversion (standardized to shipboard velocity measurements) were too high. The mistie between the synthetic seismogram and the seismic data using this method suggests that the physical properties velocity measurements for this site are not representative of in situ conditions and that the sonic log measurements should be used in constructing the synthetics.

The discrepancy between the laboratory velocity measurements and sonic log measurements at Site 1001 is problematic. Previous studies have shown that shipboard laboratory velocity measurements are often lower than sonic log measurements because of removal of overburden pressure (Hamilton, 1979; Fulthorpe et al., 1989; Urmos et al., 1993). It is unclear exactly why the laboratory velocity measurements would be higher than the in situ sonic log measurements. One possible reason for laboratory measurements being higher than log measurements could be the result of a sampling bias. In some cases, the laboratory velocity measurements were taken on core intervals having more consolidated sediment. This sampling bias favoring

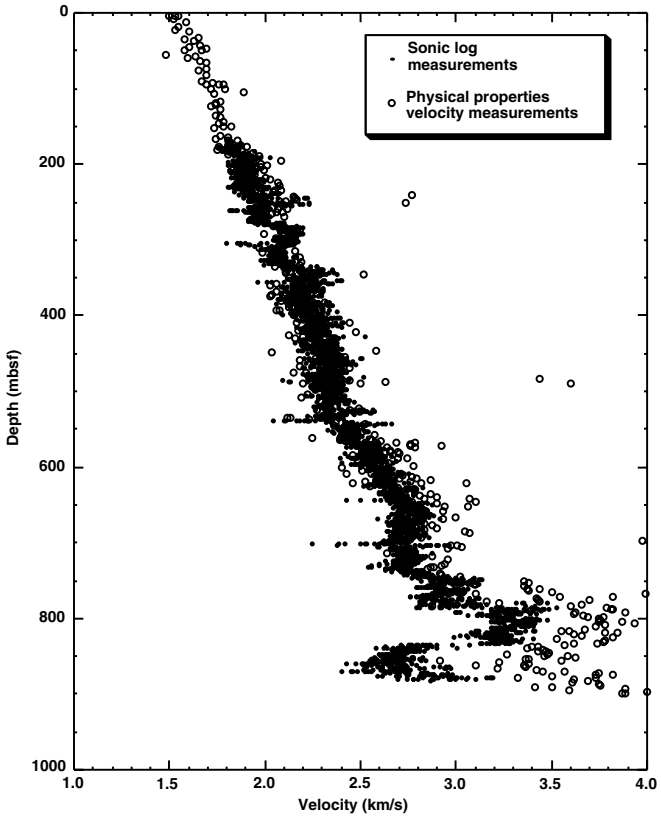

Figure 2. Sonic log and physical properties velocity measurements for Site 998.

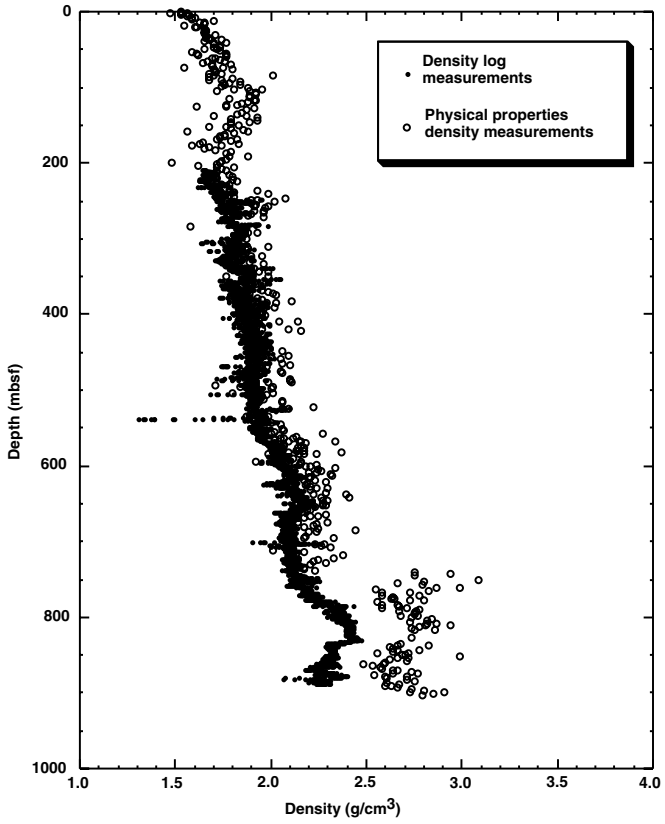

Figure 3. Density log and physical properties density measurements for Site 998.

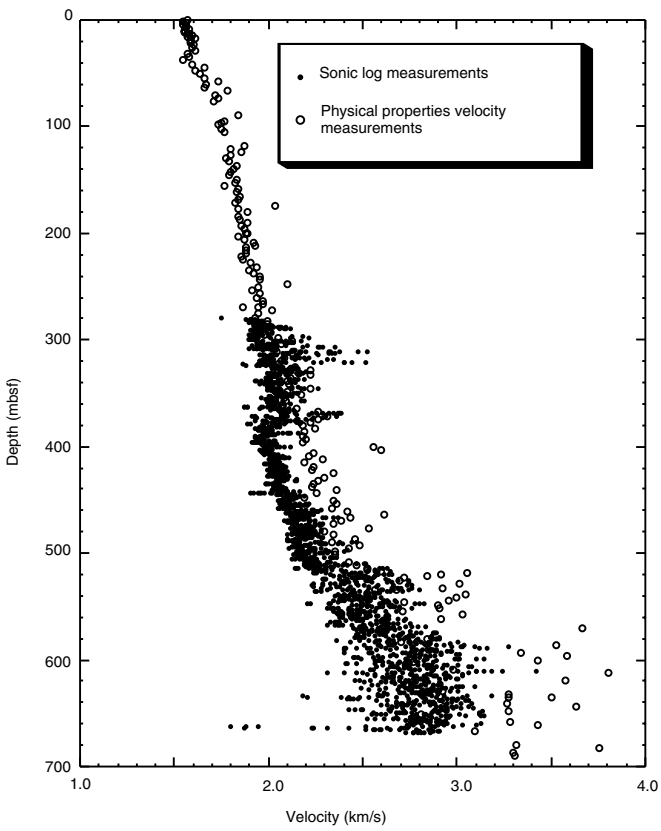

Figure 4. Sonic log and physical properties velocity measurements for Site 1000.

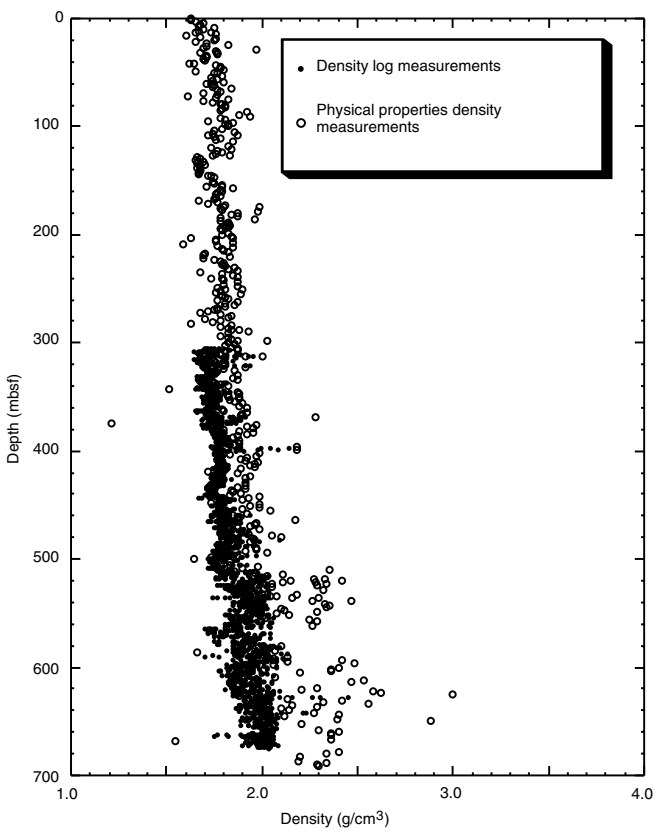

Figure 5. Density log and physical properties density measurements for Site 1000.

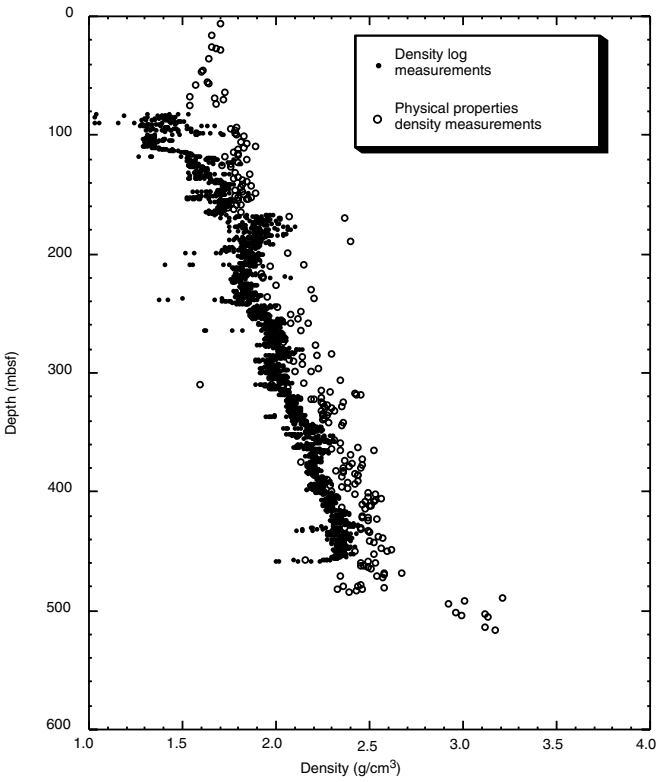

Figure 6. Density log and physical properties density measurements for Site 1001.

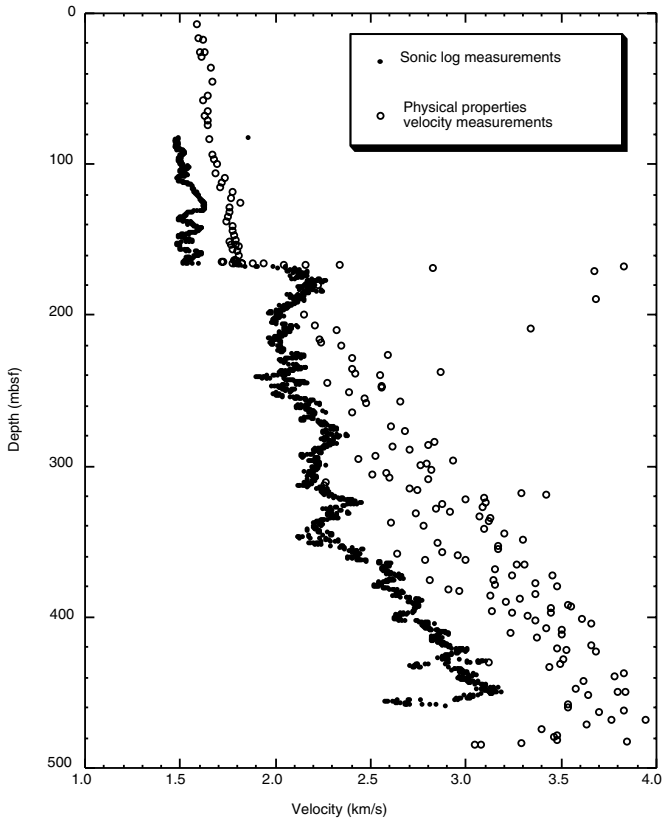

Figure 7. Uncorrected sonic log and physical properties velocity measurements for Site 1001.

measurements of more consolidated sediment may occur when shipboard scientists attempt to avoid sampling a core interval that appears to be contaminated by mudcake. The more consolidated intervals may not be representative of the gross lithology and may cause the laboratory velocity measurements to be higher than those of the actual sedimentary section. The sonic log measurements are made through transducers and receivers separated by 0.91–3.66 m (Sigurdsson, Leckie, Acton, et al., 1997). Measurements made over this distance may more accurately represent the gross lithology and in situ conditions.

Downhole log measurements are not available for the top and bottom portions of the hole. To compensate for this, velocity and density profiles were created in which core-derived velocity and density measurements are spliced to the tops and bottoms of the sonic and density logs to construct the profiles. Synthetic seismograms are created from these velocity and density profiles that extend from the seafloor to near the base of the hole. The edited velocity and density profiles used for creating the synthetic seismograms are shown in Figures 9, 10, 11, 12, 13, and 14.

Generation of the synthetic seismograms was performed using the Landmark "SynTool" module. In creating a synthetic seismogram, SynTool permits the interpreter to tie time data (the seismic data) to depth data (the well data) by integrating over the velocity profile. An impedance log and reflection coefficient are generated from the velocity and density profiles. The reflection coefficients are convolved with a seismic wavelet to produce a synthetic seismic trace. A bandpass filter (25–50–200–400 Hz) and 200-ms AGC are applied to the synthetic trace to mimic the processing of the SCS data. In this case, the seismic wavelet is obtained using a wavelet extraction from SCS data in each study area having a "clean" seafloor reflection. The synthetic seismograms are sampled at 1 ms to match the sample rate of the SCS data. The synthetic seismogram is then compared with the actual seismic traces at the drill site. The trace at the drill site was compared with adjacent traces to assure that it was representative of that part of the seismic section. Figures 15, 16, and 17 illustrate the relationship between the impedance logs, reflection coefficients, SCS traces, and synthetic traces for Sites 998, 1000, and 1001.

SITE 998

Site 998 is located in 3190.7 m of water on a plateau-like feature on the Cayman Rise, bordered by the Yucatan Basin to the north and the Cayman Trough to the south. Drilling during ODP Leg 165 recovered a largely complete lower Eocene to Pleistocene sedimentary section composed of ooze, chalk, clay, limestone, turbidites, and ash layers (Sigurdsson, Leckie, Acton, et al., 1997). Penetration at Site 998 reached 904.8 mbsf, and the hole was logged from ~180 to 880 mbsf. SCS reflection Line EW9417-13 crossed Site 998 at Shotpoint 348.

Some intervals from the synthetic seismogram do show excellent agreement with the SCS data. Reflectors from SCS Line EW9417-13 that correlate with the synthetic seismogram include those at 4280, 4355–4405, 4475, 4480, 4500, 4515, 4600–4615, 4630, 4730, 4750, 4765, and 4940–5020 ms (Fig. 18). Figure 18 also illustrates the age-depth relationship of the section cored at Site 998.

The synthetic seismogram permits correlation of the seismic data with core lithologies recovered during drilling. Several lithologic units were defined for ODP Site 998 (Sigurdsson, Leckie, Acton, et al., 1997). Unit I consists of nannofossil ooze with foraminifers and clays interbedded with graded foraminifer ooze and volcanic ash layers. Subunit IIA contains clayey nannofossil mixed sediment interbedded with turbidites and ash layers. Subunit IIB has nannofossil

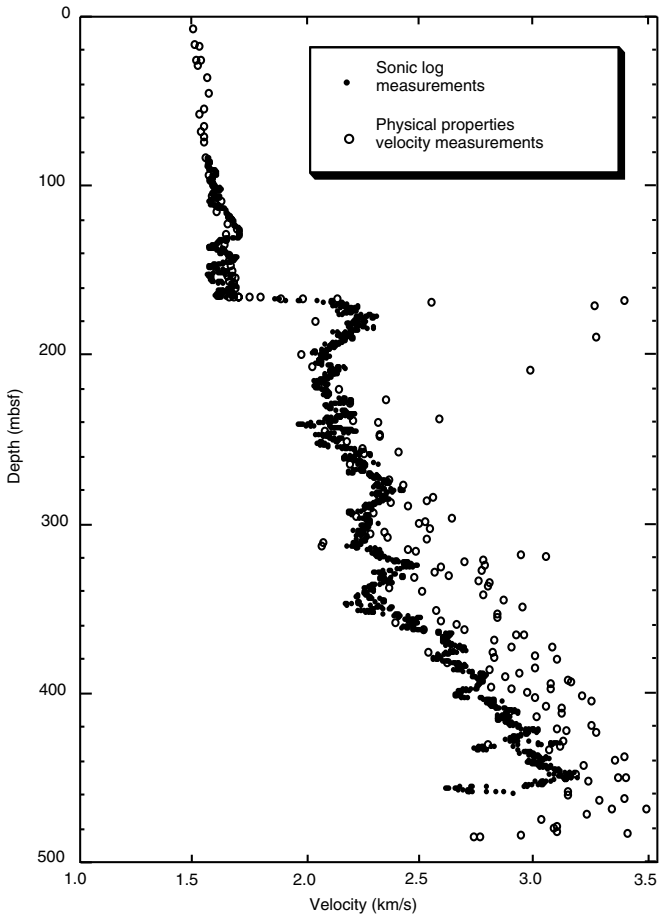

Figure 8. Modified sonic log and physical properties velocity measurements for Site 1001.

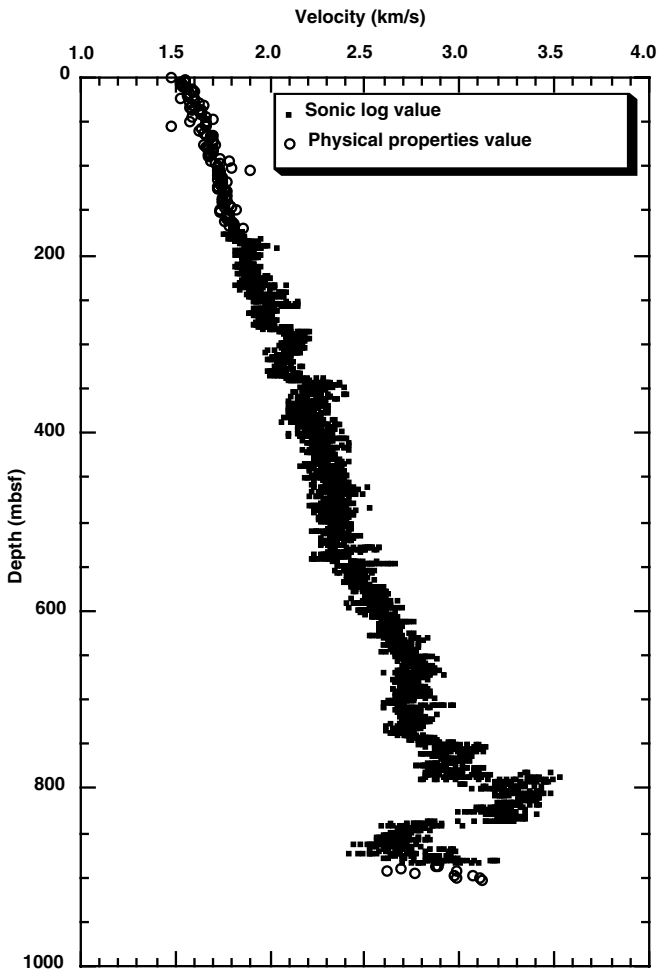

Figure 9. Site 998 composite velocity profile containing edited sonic log and physical properties velocity values used for creating the Site 998 synthetic seismogram.

ooze with foraminifers and clays interbedded with turbidites and ash layers. Subunit IIC contains clays with nannofossils to nannofossil mixed sediment interbedded with turbidites and ash layers. Unit III contains nannofossil chalk with clays, interbedded with foraminifer chalk with clay, altered volcanic ash layers, and chert. Unit IV has calcareous volcaniclastic mixed sedimentary rock interbedded with altered volcanic ash with carbonates.

Figure 19 illustrates the core lithologies and lithostratigraphic units that elicit responses in the SCS data that are distinct from units and lithologies above and below them. The interval from 30 to 120 mbsf correlates with a zone of lower amplitude and less continuous reflections. This interval is also associated with an interval of increased turbidite thickness compared to the underlying section. Lithostratigraphic Subunits IIB and IIC correlate with a zone of high frequency, high amplitude, and highly continuous reflections. Unit IV is marked by a set of low-frequency, high-amplitude, moderately continuous reflections.

In addition to the correlation of these units with the seismic data, several other lithologic intervals appear to correlate with the seismic data. Chert layers present in the core at 250, 350, 680, 730, 800, and 880 mbsf appear to correlate with moderate- to high-amplitude, moderately continuous reflectors. Unfortunately, chert layers at 465, 495, 520, 570, and 605 mbsf do not appear to correlate with any significant seismic reflectors. The lack of a seismic response may be a result of thin chert layers. Turbidite-rich intervals from 30 to 120, 180 to 260, 470 to 510, and 610 to 680 mbsf correlate with zones of lower amplitude, less continuous reflectors compared to intervals above and below the turbidite-rich intervals. Aside from the chert and turbidite-rich intervals, the relatively homogenous sediment recovered at Site 998 does not have significant variations in the physical properties that might cause a change in seismic response.

SITE 1000

Site 1000 is located in 927.2 m of water in Pedro Channel along the northern Nicaraguan Rise. The northern Nicaraguan Rise is bordered by the Cayman Trough to the north and the southern Nicaraguan Rise and Colombian Basin to the south. Pedro Channel is the widest and deepest channel along the east-northeast trending Nicaraguan Rise. Shallow-water (30 m) carbonate banks bound Pedro Channel on three sides. These banks include Pedro Bank to the east, Rosalind Bank to the west, and Serranilla Bank, Alice Shoal, and Banco Nuevo to the south. A largely complete 695.6-m section of Miocene to Holocene sediment was recovered at Site 1000. This sediment consists predominantly of periplatform ooze, chalk, and limestone. Site 1000 was logged from 277 to 675 mbsf. SCS reflection Line CH9204-30 crosses Site 1000 at Shotpoint 1495.

The synthetic seismogram shows very good agreement with the seismic data, and thus provides a link between the seismic sections

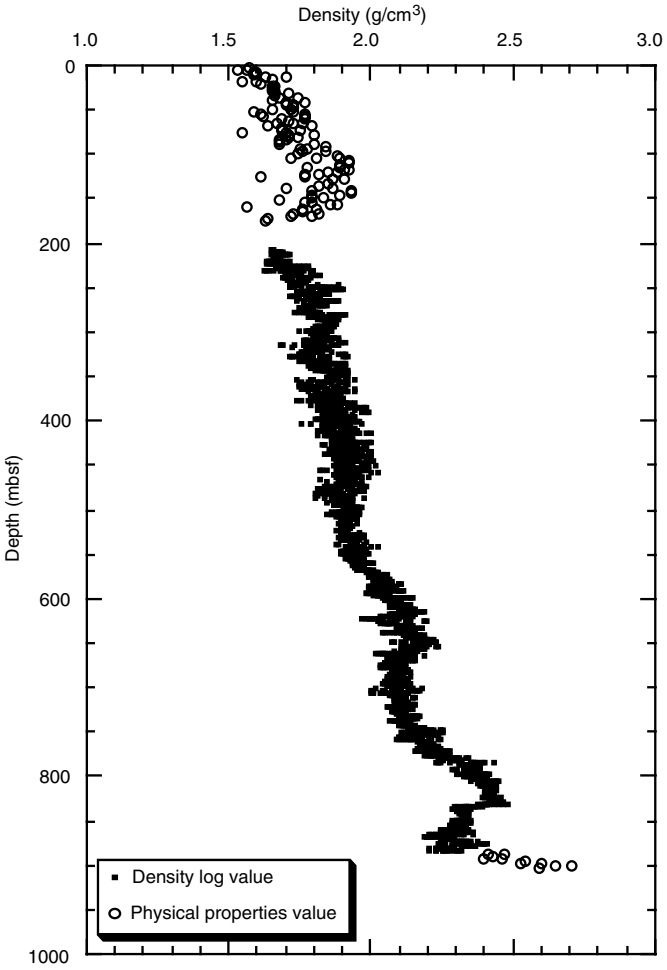

Figure 10. Site 998 composite density profile containing edited density log and physical properties density values used for creating the Site 998 synthetic seismogram.

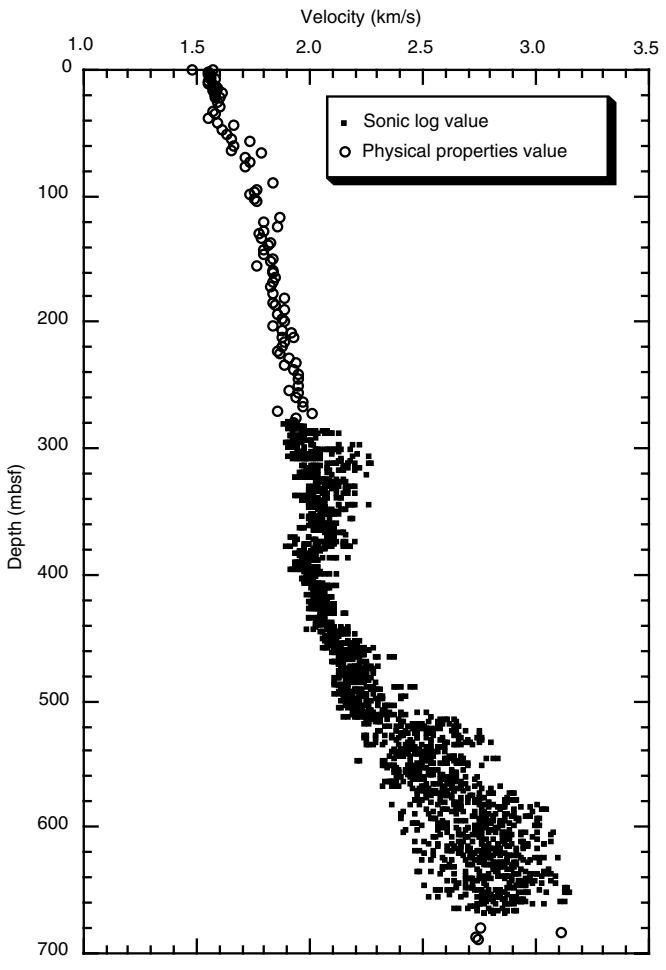

Figure 11. Site 1000 composite velocity profile containing edited sonic log and physical properties velocity values used for creating the Site 1000 synthetic seismogram.

and the core data. This link provides critical information about how the core lithologies relate to the seismic facies, as well as age control for the correlated seismic horizons (~0–700 milliseconds below seafloor [ms bsf]). The main seismic event used for correlation is a set of high-amplitude reflections starting at 320 ms bsf or a two-way traveltime (TWT) of 1570 ms. In addition to these events, reflectors at 1435, 1520, 1640, 1720, 1760–1780, and 1870–1900 ms correlate reasonably well between the synthetic trace and the SCS data (Fig. 20).

Figure 20 illustrates correlation between SCS Line CH9204-30 and the synthetic-generated traces. Based on this correlation, several characteristics of the ODP Site 1000 core can be correlated with the seismic data. Several lithologic units were defined for Site 1000 (Fig. 21; Sigurdsson, Leckie, Acton, et al., 1997). Subunit IA consists of nannofossil and micritic oozes with foraminifers and pteropods. Subunit IB contains micritic nannofossil ooze with foraminifers to foraminiferal micritic ooze with nannofossils, volcanic ash layers, and normally graded turbidites. Subunit IC varies from micritic nannofossil chalk with clay and foraminifers to clayey nannofossil chalk with micrite. Subunit ID consists of micritic nannofossil chalk with foraminifers. Subunit IIA contains calcareous limestone with foraminifers to nannofossil micritic limestone with clay and foraminifers, with interbedded minor volcanic ash layers. Subunit IIB has calcareous limestone with foraminifers and nannofossil micritic limestone with clay and foraminifers, interbedded volcanic ash layers, and normally graded sandy turbidites. Of these, two units appear to elicit a distinctive response in the seismic data. Lithostratigraphic Subunit IA from 0 to 51 mbsf correlates with a seismic interval that has high-continuity reflectors (Fig. 21). Subunit IA was identified as containing more clay minerals and larger magnitude variations in carbonate content than the underlying stratigraphic subunit. It is possible that these variations could result in the seismic reflectors present over that interval. Lithostratigraphic Subunit ID from 486 to 513 mbsf also correlates with a seismically distinctive interval containing high-amplitude, high-frequency, continuous reflectors (Fig. 21). This subunit is differentiated from subunits above and below by its massive bedding and higher carbonate content.

Another interesting correlation between the core and the seismic data is at ~513 mbsf. Lithologically, this depth marks the transition from chalk to limestone. It coincides with physical properties increases in velocity and density and decreases in water content and porosity (Sigurdsson, Leckie, Acton, et al., 1997). These variations are also evident in the sonic, density, and resistivity logs from downhole measurements (Sigurdsson, Leckie, Acton, et al., 1997). Seismically, this transition is marked by the disappearance of high-frequency reflections (Fig. 21). It is likely that high-frequency energy is unable to pass far beyond this distinct lithologic boundary because of attenuation.

Despite the fact that it comprises only a small portion of the recovered sediment, the presence of turbidites in the cores also seems

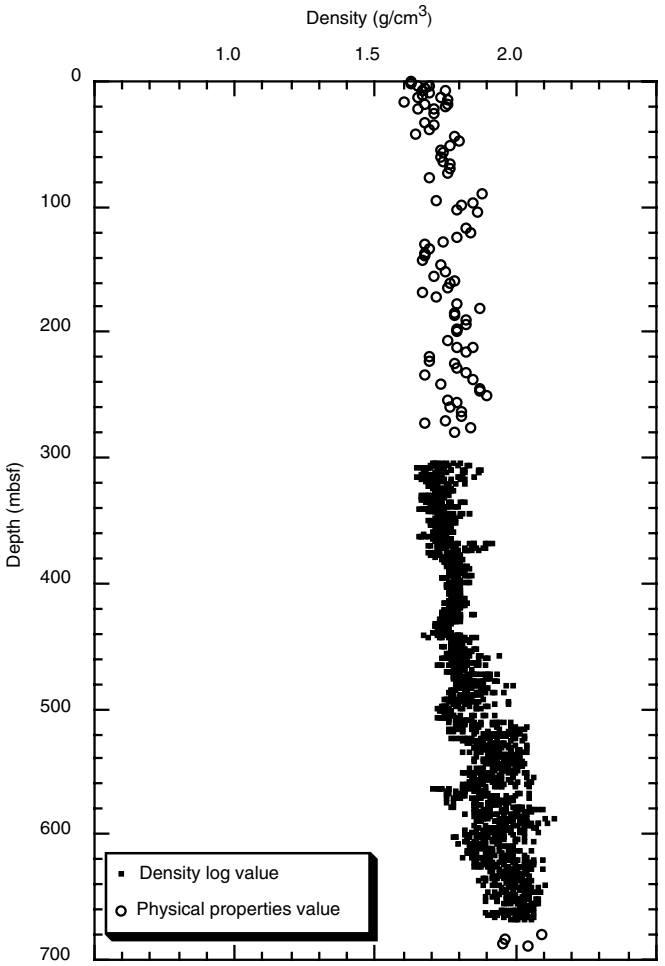

Figure 12. Site 1000 composite density profile containing edited density log and physical properties density values used for creating the Site 1000 synthetic seismogram.

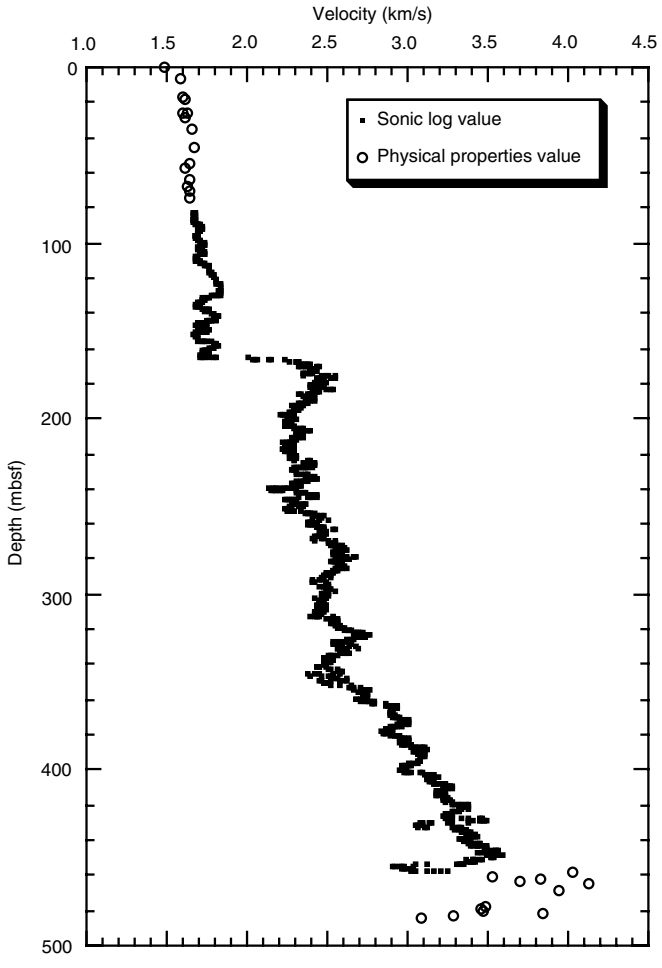

Figure 13. Site 1001 composite velocity profile containing edited sonic log and physical properties velocity values used for creating the Site 1001 synthetic seismogram.

to correlate with distinctive seismic facies. Four distinctive cored intervals contain turbidites: 60–80, 245–270, 320–340, and 591–696 mbsf. The intervals 60–80, 245–270, and 320–340 mbsf consist of planktonic foraminifer turbidites (Fig. 21). These thin- to medium-bedded turbidites (<30 cm) comprise a maximum of 3% of the core recovered in the core containing the highest number of turbidites. The planktonic foraminifer turbidite intervals correlate with a low-amplitude, lower continuity seismic facies. The interval from 591 to 696 contains coarse-grained turbidites with bank-derived foraminifers (Fig. 21). This interval correlates with a high-amplitude, locally continuous seismic facies.

The origin of the low-amplitude, lower discontinuity seismic facies that typifies the three planktonic foraminifer turbidite intervals may result from the localized disruption of the physical properties that would otherwise result in a moderate-amplitude, continuous seismic facies. The sonic and density logs across the three planktonic foraminifer turbidite intervals show minimal changes relative to the overlying and underlying turbidite-free sedimentary units. All three turbidite intervals contain pelagic material and current-winnowed, fine-grained carbonates, as do the overlying and underlying turbidite-free sedimentary units. In the turbidite-free sections, the impedance contrasts resulting in seismic reflections are often caused by variations in degree of cementation, porosity, or water content, all of which affect the velocity and density (Slowey et al., 1989). Over the turbidite intervals, however, these properties could be disrupted locally by deposition of the turbidite. This might result in the discontinuous, low-amplitude seismic response.

For intervals containing the coarse-grained, bank-derived turbidites, the case appears to be different. The turbidites tend to range in thickness from a few to several tens of centimeters, though none is >60 cm (Sigurdsson, Leckie, Acton, et al., 1997). Both the sonic and density logs show large-amplitude variations over this turbiditic interval. The seismic response is a result of the higher velocity and density values in the turbidites relative to intervals of sediment above and below without the coarse-grained turbidites. The high-amplitude seismic reflections over this interval result from the interference pattern of numerous impedance contrasts and do not represent distinct turbidite layers.

Core recovery of a significant paleoceanographic event, the "Carbonate Crash," is present between 380 and 460 mbsf (Sigurdsson, Leckie, Acton, et al., 1997). The carbonate crash is marked by a ~15% decrease in carbonate content in the sediment over this interval. The impedance log and reflection coefficient over this interval have lower amplitude variations compared with the overlying and underlying intervals (Fig. 16). This interval correlates to a zone of relatively low-amplitude reflectors on the synthetic seismogram (Fig. 20). This is evident in the CH9204 seismic data as a zone of low-amplitude to transparent seismic facies compared to the facies above and below. The high-amplitude reflector at ~440 ms TWT on Trace 1495 (Fig. 16) does not correlate well with the synthetic seismogram. The source of this reflector remains unidentified.

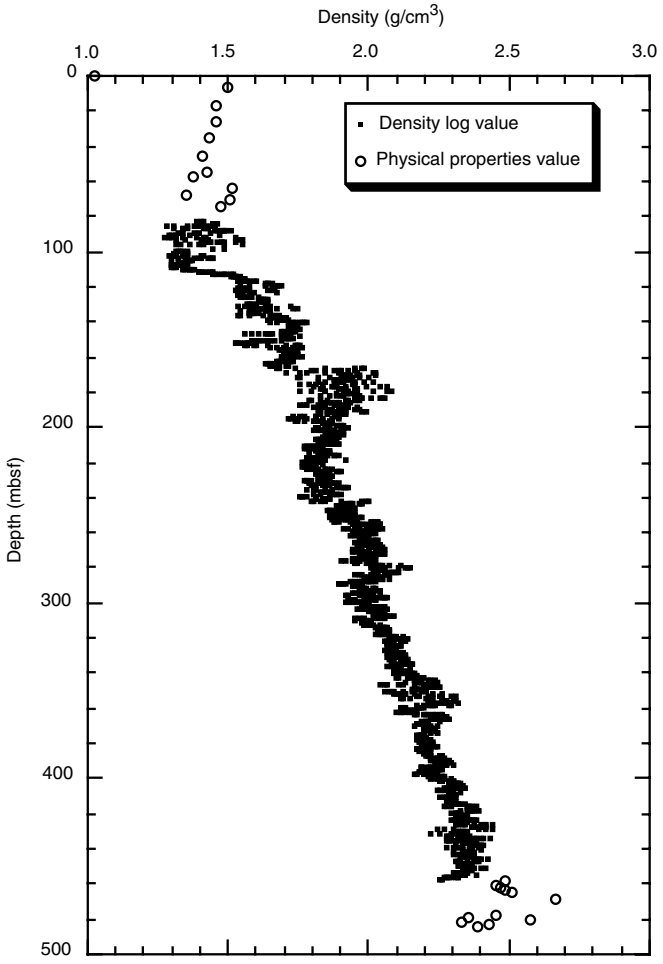

Figure 14. Site 1001 composite density profile containing edited density log and physical properties density values used for creating the Site 1001 synthetic seismogram.

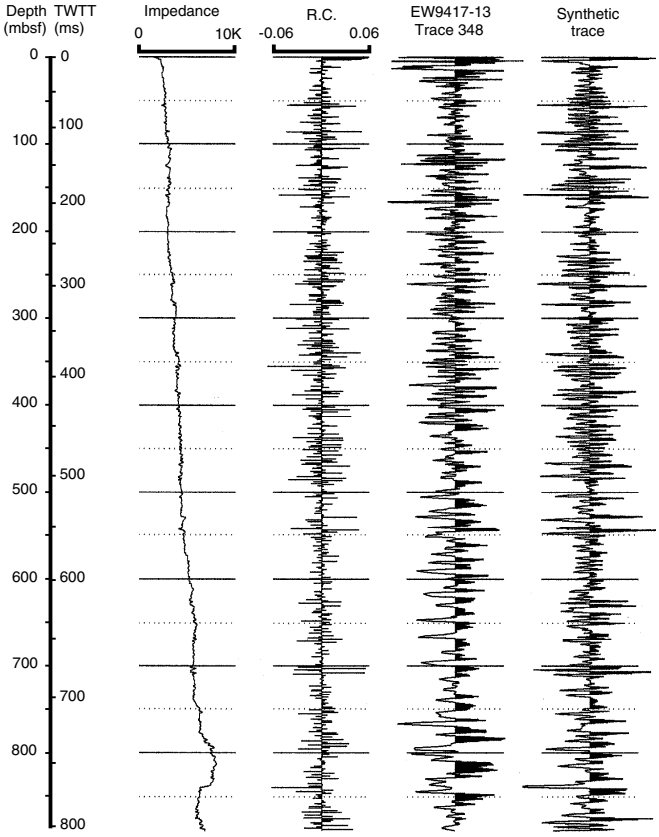

Figure 15. Site 998 depth-TWT relationship with linear depth scale. Included are the impedance log, reflection coefficient, Trace 348 from SCS Line CH9417-13, and synthetic seismogram generated using the velocity and density profiles.

Several lithologic facies in the core do not appear to have any visible effect on either the synthetic seismogram or the seismic facies. Numerous ash layers were recovered from Site 1000, with a maximum thickness of 53 cm, but typically much thinner with a 5.1-cm mean thickness (Sigurdsson, Leckie, Acton, et al., 1997). Most notably, these ash layers show peak accumulation rates over intervals 280–300, 510–540, and 600–696 mbsf. None of the intervals containing ash layers have an effect on the velocity or density that would affect a seismic response.

There is a significant event in the seismic (1570–1600 ms TWT), synthetic (330–350 ms TWT), and log data (295–320 mbsf) that does not appear to correlate with any major lithologic properties. The logs over this interval show widely varying values for the sonic, density, photoelectric effect, and gamma-ray logs compared to units above or below this interval. The variation is also evident in the impedance log and reflection coefficient (Fig. 16). The seismic response is a series of high-amplitude, high-frequency, high-continuity, parallel reflectors (Fig. 21).

SITE 1001

Site 1001 is located in 3271.0 m of water on the edge of the Southern Nicaraguan Rise, just north of the Hess Escarpment. ODP drilling at Site 1001 recovered a 522.8-m section composed of clay, ooze, chalk, limestone, chert, and basalt (Sigurdsson, Leckie, Acton, et al., 1997). The recovered sediment consists of a middle Miocene to Pleistocene section overlying a Cretaceous to upper Eocene section, separated by an unconformity. The section was logged from 83 to 470 mbsf. SCS reflection Line EW9417-10 crossed Site 1001 at Shotpoint 1500. Two major Caribbean seismic reflectors, A" and B", have been mapped throughout the Site 1001 site survey (Cunningham, 1998). These horizons were penetrated at Deep Sea Drilling Project Site 152, located roughly 40 km east-northeast of Site 1001 (Edgar, Saunders, et al., 1973). Although recovery at Site 152 was poor, the A" horizon was correlated with lower Eocene chalks with minor chert or silicified cherty Paleocene limestone. The B" horizon with associated with Upper Cretaceous basalt.

The synthetic seismogram at Site 1001 facilitates correlation of the core data with the SCS data. Reflectors within the SCS data that appear to correlate with the synthetic seismogram include those at 2350, 2410, 2440–2465, 2520, 2540, 2775, and 2790 ms. Figure 22 illustrates the correlation between the synthetic seismogram and core-derived depths and ages.

The primary objective of creating synthetic seismograms over Site 1001 was to correlate the Eocene-Miocene unconformity identified in the core with the A" reflector and the basaltic crust with the acoustic basement or B" reflector interpreted in the seismic data (Fig 23). The A" reflector is clearly evident on both the seismic data from SCS Line EW947-10 at 2540 ms and the synthetic seismogram as the largest peak in the synthetic. The other significant correlation is the end of the synthetic seismogram at 2805 ms with basement recovered at 485 mbsf. The end of the synthetic seismogram correlates with the top of basalt recovered in the core, and the B" basement horizon from the SCS interpretation (Cunningham, 1998). One interesting note is the lack of any seismic response at the chalk to limestone transition (lithostratigraphic Units II to III) as was evident in the Site 1000 SCS

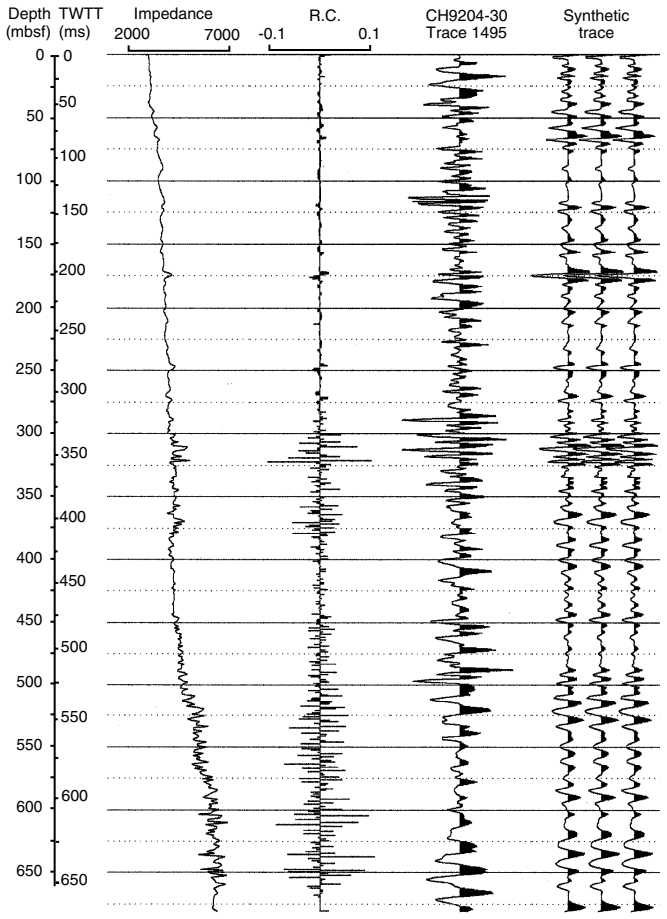

Figure 16. Site 1000 depth-TWT relationship with linear depth scale. Included are the impedance log, reflection coefficient, Trace 1495 from SCS Line CH9204-30, and synthetic seismogram generated using the velocity and density profiles.

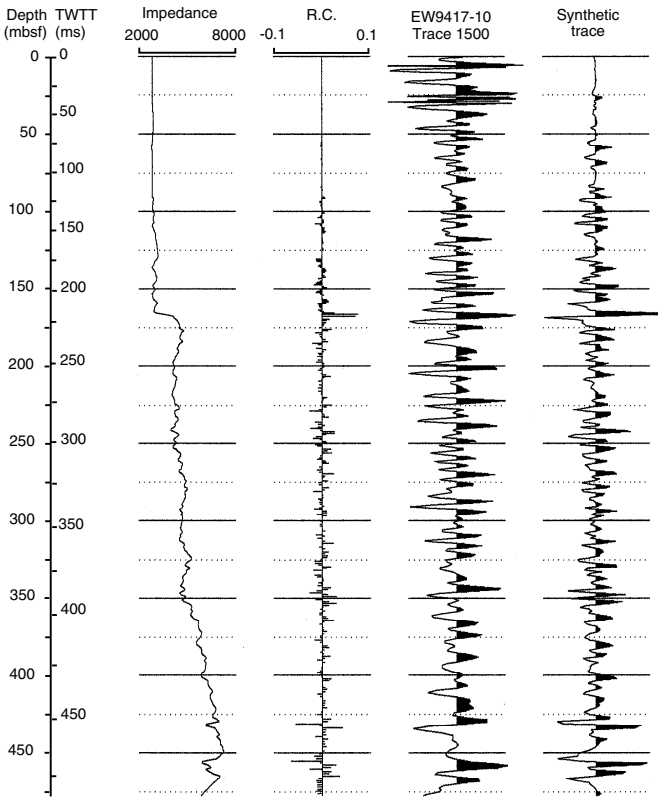

Figure 17. Site 1001 depth-TWT relationship with linear depth scale. Included are the impedance log, reflection coefficient, Trace 1500 from SCS Line CH9417-10, and synthetic seismogram generated using the velocity and density profiles.

data and synthetic seismogram. The absence of a major change in the impedance across this interface at Site 1001 results in the lack of a seismic response.

Chert layers were recovered in core from Site 1001 at ~166, 200, 240, 295, and 450–470 mbsf; however, none of these appears to have any impact on the velocity profile at this site (Fig. 13). The chert layers at ~166 mbsf are also associated with the lower Eocene to middle Miocene unconformity. Both the velocity and density measurements increase from the Miocene section into the Eocene. The changing physical properties of the Miocene and Eocene sediment rather than the presence of chert causes the impedance contrast created across this boundary. In most cases, the chert layers are so thin that they have minimal effect on the sonic and density logs across those intervals. Without a velocity or density change in the logs, there is no impedance contrast and the cherts have no effect on the synthetic seismogram.

PROBLEMS IN MATCHING CORE TO SEISMIC

There are numerous reasons why synthetic seismograms do not tie precisely with the actual seismic data. The most common reasons are problems with the velocity model. In this study, the sonic log and physical properties velocity measurements were used to calculate the two-way traveltime-depth relationship. There are several factors that might affect the accuracy of the sonic log, and thus the time-depth relationship. If the borehole becomes washed out, the sonic log will not read true rock formation velocities. If the formation is anisotropic, the seismic wave energy will not necessarily travel in the same direction as the log measurements. Dispersion effects can cause a poor correlation between the seismic data and the synthetic trace. Ideally, check-shot surveys or vertical seismic profiles would be used to refine the time-depth curve, as well as gain information on formation anisotropy and frequency transmission along the borehole. Unfortunately, this data was not available for this study. As mentioned previously, shipboard velocity measurements may be erroneous because of the removal of overburden pressure (Hamilton, 1979; Fulthorpe et al., 1989; Urmos et al., 1993).

Attempting to tie the synthetic seismograms to single-channel seismic data also causes problems. Single-channel seismic data often have artifacts that do not accurately represent the subsurface geology. Multiples and intramultiples in the seismic data are present in the SCS data and are extremely difficult to remove. SCS data are also highly susceptible to being affected by out-of-plane energy. These artifacts in the seismic data are not recreated in the synthetic seismogram and could affect the correlation. Another problem with SCS data is that the data have no far-offset stacking to help remove random noise from the recorded trace. In such a case, the major reflectors in the seismic data will typically match with the synthetic trace. This noise, however, is impossible to accurately model with synthetic seismograms and can have a significant effect on lowering the correlation coefficient. This is believed to be one of the major reasons for the low correlation coefficients of the synthetic seismograms generated in this study.

There are several other potential reasons that the synthetic might not tie with the real seismic trace. A deviated borehole would cause the drillhole to appear deeper than it actually is, thus causing events in the synthetic to appear “deeper” than those in the seismic data. De-

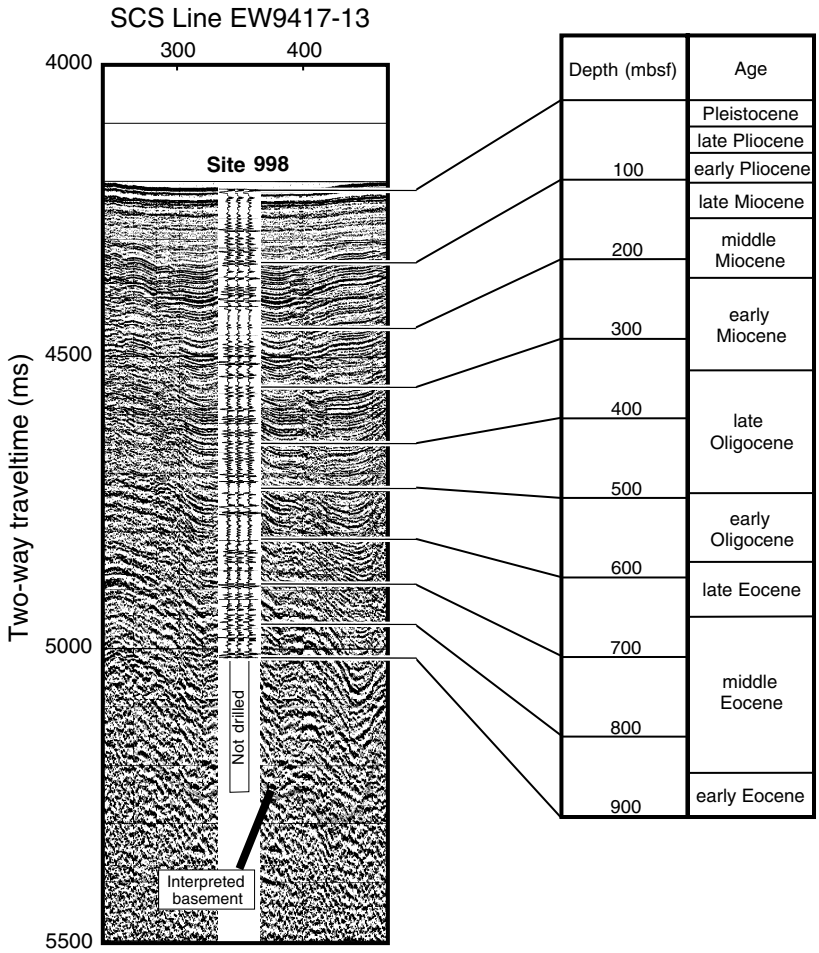

Figure 18. Overlay of synthetic seismogram and SCS Line EW9417-13 at Site 998, with depth and age boundaries.

spite using the seismic wavelet extraction procedure, the lack of an actual source wavelet could cause differences between the synthetic seismogram and seismic data. Finally, as mentioned earlier, there are numerous factors that could affect the quality of the sonic and density logs as well as the physical properties data, any of which could adversely affect the resultant synthetic seismogram. Unfortunately, these effects are difficult to quantify.

SUMMARY

Correlation of SCS data and ODP core lithologies recovered at Sites 998, 1000, and 1001 was accomplished by creating synthetic seismograms from velocity and density measurements. At all three sites, many of the major reflectors in the SCS data correlate with high-amplitude events in the synthetic seismograms. Furthermore, vertical changes in SCS facies can be related to downhole variations in core lithologies.

The synthetic seismogram generated for Site 998 permits correlation of the Site 998 core with SCS data over the site. Several of the units identified in the lithostratigraphic descriptions from Site 998 (Sigurdsson, Leckie, Acton, et al., 1997) correlate quite well with seismic intervals having distinctive seismic character. Zones of low-continuity, low-amplitude seismic facies correlate with several turbidite-rich core intervals. Several chert layers correlate with moderate- to high-amplitude, moderate- to high-continuity reflections. However, some intervals of chert layers cause no seismic response.

The synthetic seismogram results from Site 1000 also provide excellent visual correlation with SCS data from Line CH9204-30. The correlation with the biostratigraphy from the core permits age determination of interpreted seismic horizons. The synthetic seismogram also correlates several seismic characteristics with lithologies from Site 1000. Several planktonic foraminifer turbidites correlate with zones of low continuity seismic reflectors. An interval of coarse-grained, neritic sand turbidites correlates with high-amplitude, moderately continuous reflectors. Finally, the chalk-limestone transition is correlated with a high-amplitude reflection, below which there are no high-frequency reflections.

The synthetic seismogram created for Site 1001 facilitates correlation between the SCS data and the core recovered from Site 1001. The most significant correlation links the 30-Ma middle Miocene to early Eocene unconformity in the core with the A" seismic reflector and the sediment-basement interface with the B" seismic reflector. Several chert layers identified in the ODP core do not correlate with SCS reflectors.

ACKNOWLEDGMENTS

We would like to thank Gary Acton, Tobias Moerz, and anonymous reviewers for their constructive insight in reviewing this manuscript. We thank the crews and scientists aboard the *Cape Hatteras*, *Maurice Ewing*, and *JOIDES Resolution* and at the Lamont-Doherty Earth Observatory for their efforts in the acquisition and processing of the data used in this study. The senior author wishes to thank Amoco Exploration and Production Company (Alan Brown and Margaret Keillor) for providing access and support for use of the Landmark software and workstations necessary to complete this study. This re-

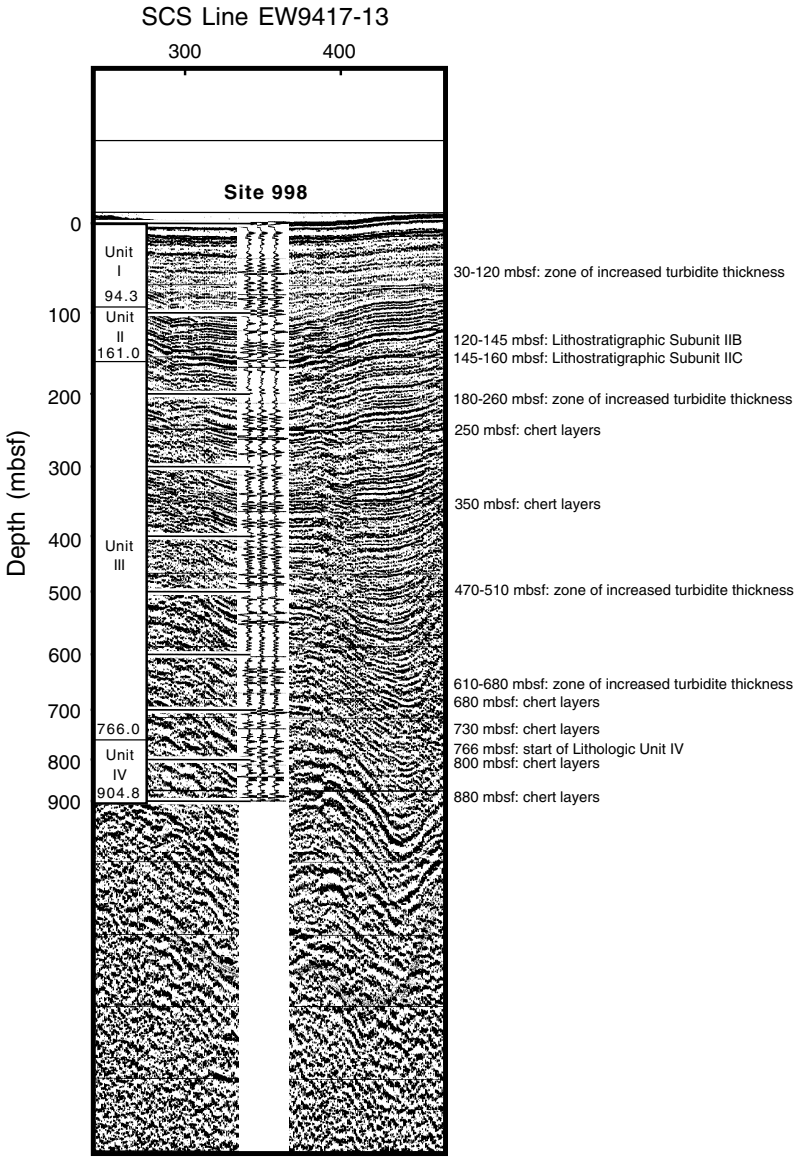

Figure 19. Correlation of Site 998 lithostratigraphic units and core lithologies with SCS Line EW9417-13.

search comprises part of the doctoral dissertation of the senior author (Cunningham, 1998) and was supported by JOI/USSP/TAMRF Grants No. F000307 and F000395.

REFERENCES

Carlson, R.L., Gangi, A.F., and Snow, K.R., 1986. Empirical reflection travel time versus depth and velocity versus depth functions for the deep-sea sediment column. *J. Geophys. Res.,* 91:8249–8266.

Cunningham, A.D., 1998. The Neogene evolution of the Pedro Channel carbonate system, northern Nicaragua Rise [Ph.D. thesis]. Rice Univ., Houston.

Edgar, N.T., Saunders, J.B., et al., 1973. *Init. Repts. DSDP,* 15: Washington (U.S. Government Printing Office).

Fulthorpe, C.S., Schlanger, S.O., and Jarrard, R.D., 1989. In situ acoustic properties of pelagic carbonate sediments on the Ontong Java Plateau. *J. Geophys. Res.,* 94:4025–4032.

Hamilton, E.L., 1979. Sound velocity gradients in marine sediments. *J. Acoust. Soc. Am.,* 65:909–922.

Sigurdsson, H., Leckie, R.M., Acton, G.D., et al., 1997. *Proc. ODP, Init. Repts.,* 165: College Station, TX (Ocean Drilling Program).

Slowey, N.C., Neumann, A.C., and Baldwin, K.C., 1989. Seismic expression of Quaternary climatic cycles in the periplatform carbonate ooze of the northern Bahamas. *Geol. Soc. Am. Bull.,* 101:1563–1573.

Urmos, J., Wilkens, R.H., Bassinot, F., Lyle, M., Marsters, J.C., Mayer, L.A., and Mosher, D.C., 1993. Laboratory and well-log velocity and density measurements from the Ontong Java Plateau: new in-situ corrections to laboratory data for pelagic carbonates. *In* Berger, W.H., Kroenke, L.W., Mayer, L.A., et al., *Proc. ODP, Sci. Results,* 130: College Station, TX (Ocean Drilling Program), 607–622.

Date of initial receipt: 24 June 1998
Date of acceptance: 29 April 1999
Ms 165SR-024

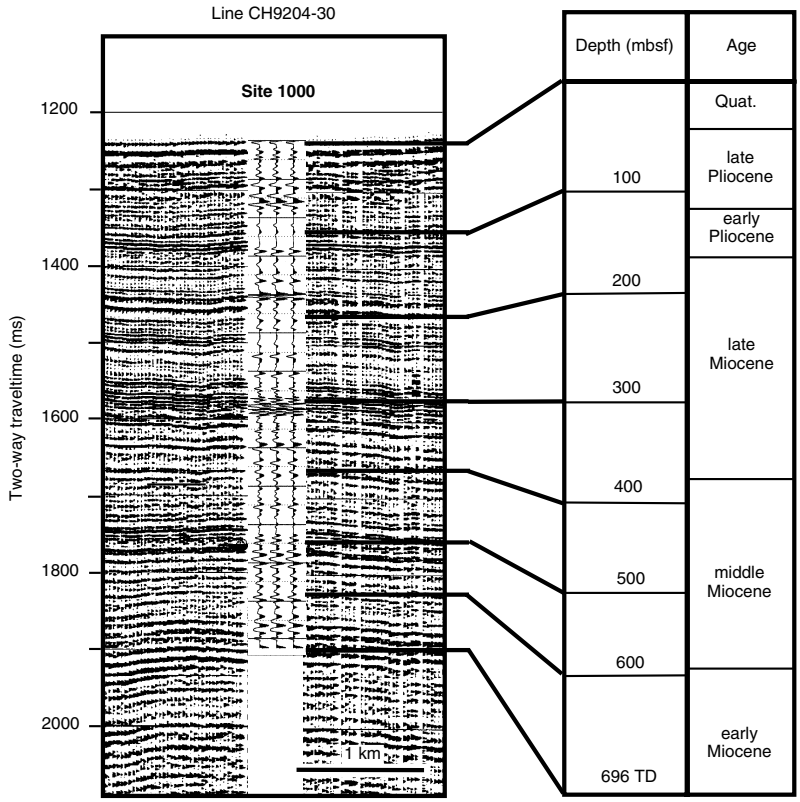

Figure 20. Overlay of synthetic seismogram and SCS Line CH9204-30 at Site 1000, with depth and age boundaries.

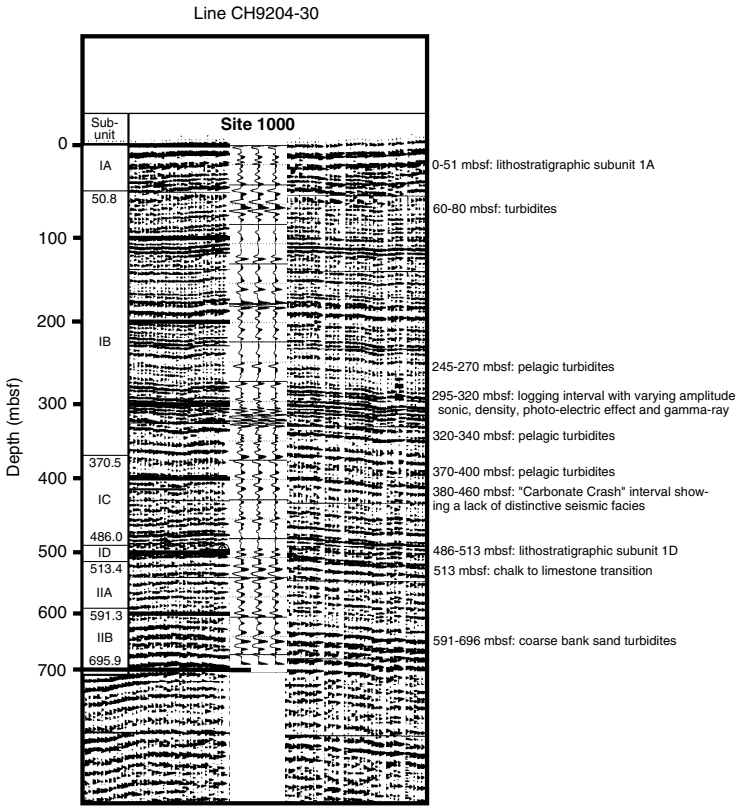

Figure 21. Correlation and noncorrelation of several lithologic events from Site 1000 with SCS Line CH9204-30.

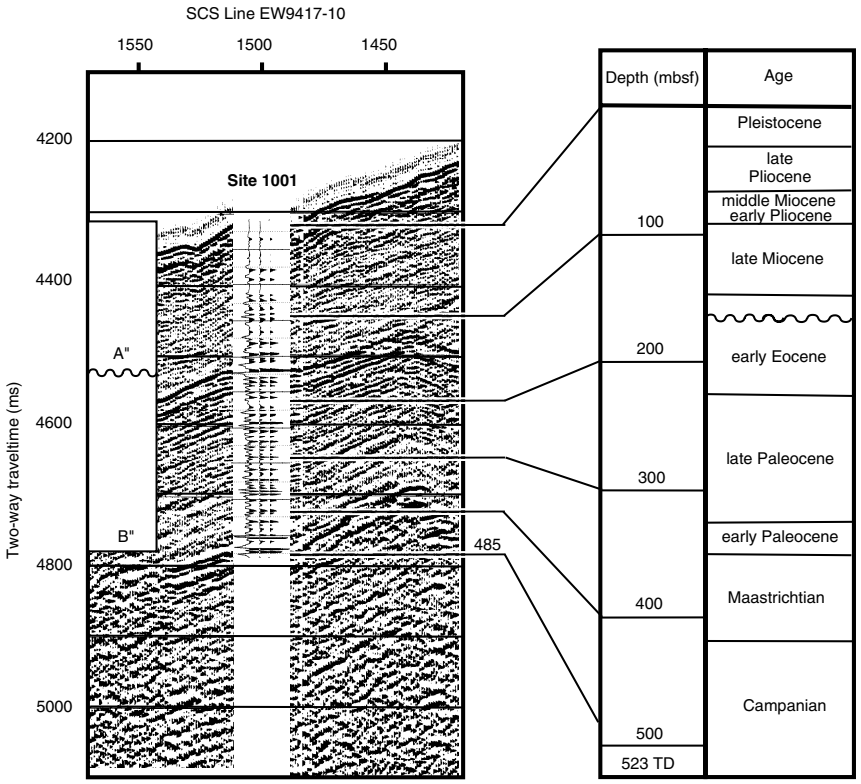

Figure 22. Overlay of synthetic seismogram and SCS Line EW9417-10 at Site 1001, with depth, age boundaries, and Horizons A" and B".

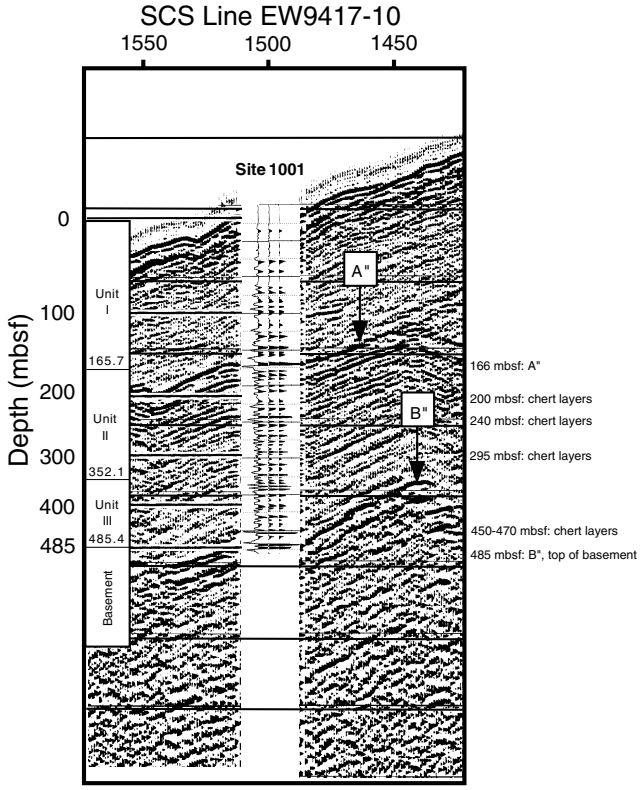

Figure 23. Correlation of Site 1001 lithostratigraphic units and core lithologies with SCS Line EW9417-10.